Geophysical Research Letters

RESEARCH LETTER
10.1029/2023GL102940

Disposal From In Situ Bitumen Recovery Induced the M_L 5.6 Peace River Earthquake

Ryan Schultz[1], Jeong-Ung Woo[1], Karissa Pepin[1], William L. Ellsworth[1], Howard Zebkar[1], Paul Segall[1], Yu Jeffrey Gu[2], and Sergey Samsonov[3]

[1]Department of Geophysics, Stanford University, Stanford, CA, USA, [2]Department of Geophysics, University of Alberta, Edmonton, AB, Canada, [3]Canada Centre for Mapping and Earth Observation, Natural Resources Canada, Ottawa, ON, Canada

Key Points:

- On 30 November 2022 one of Alberta's largest recorded events (M_L 5.6, M_W 5.1) occurred in a region of in situ bitumen recovery
- A well oriented fault was reactivated with reverse slip (29 cm), causing up to 3.4 cm of ground deformation
- The event was likely induced by pore pressure from disposal, with smaller poroelastic stress changes from bitumen production

Supporting Information:

Supporting Information may be found in the online version of this article.

Correspondence to:

R. Schultz,
rjs10@stanford.edu

Citation:

Schultz, R., Woo, J.-U., Pepin, K., Ellsworth, W. L., Zebkar, H., Segall, P., et al. (2023). Disposal from in situ bitumen recovery induced the M_L 5.6 Peace River earthquake. *Geophysical Research Letters*, *50*, e2023GL102940. https://doi.org/10.1029/2023GL102940

Received 18 JAN 2023
Accepted 26 FEB 2023

Author Contributions:

Conceptualization: Ryan Schultz, William L. Ellsworth
Data curation: Ryan Schultz, Jeong-Ung Woo, Karissa Pepin, William L. Ellsworth, Howard Zebkar, Yu Jeffrey Gu, Sergey Samsonov
Formal analysis: Ryan Schultz, Jeong-Ung Woo, Karissa Pepin, William L. Ellsworth, Howard Zebkar, Paul Segall
Funding acquisition: William L. Ellsworth
Investigation: Ryan Schultz
Methodology: Ryan Schultz, Jeong-Ung Woo, Karissa Pepin, William L. Ellsworth, Paul Segall

Abstract Earthquakes induced by human activities can impede the development of underground resources. Significant induced events (M5) have caused both economic and human losses. The recent M_L 5.6 (M_W 5.1) event near Peace River, Alberta occurs in a region of in situ bitumen recovery. We find that 3.4 cm of ground deformation was caused by reverse fault slip (~29 cm), possibly related to Peace River Arch faulting. Events are located within the shallow basement, nearby to significant wastewater injection into Paleozoic strata. We find a statistical relationship between earthquakes and injection operations. These events were likely related to the in situ bitumen development: dominantly from wastewater disposal induced pore pressure increases, with smaller poroelastic contributions from bitumen recovery. The assessment of this earthquake as induced will likely have implications for future energy development, management, and regulation—including carbon capture and blue hydrogen.

Plain Language Summary Earthquakes can be caused by underground fluid injection; cases of M5 induced events have caused damage and harm. One of the largest recorded earthquakes in Alberta (M_L 5.6) occurred in a region of underground oil sand development. Here, ground shaking and deformation information are combined into an interpreted result: that ancient faults were reactivated with reverse slip. The fault slip is largely within the crystalline basement, with a small portion extending into basal sediments. Nearby injection operations dispose of petroleum-related wastewater in these basal sediments. This earthquake was likely triggered by the injection process: injection increases pore pressure, which diffuses laterally along permeable sediments, until encountering fractured rock, which channelizes flow into the crystalline basement—the increase of pore pressure within the fault continues until reaching a critical point for slip initiation. This event likely being induced will have important implications for future operations.

1. Introduction

The 30 November 2022 earthquake near the town of Peace River (~45 km ESE) is one of the largest documented (M_L 5.6) in the history of Alberta (Figure 1), exceeded by the M_W 5.4 14 March 2001 Dawson Creek event. The Peace River event was widely felt: ~690 km SSE in the city of Calgary and ~340 km WNW at Fort McMurray (NRCan ID: 20221130.0055; USGS ID: us6000j5n4). So far, no damage has been reported; likely because of the remote setting of the epicenter (Schultz et al., 2021b). Statements by the Alberta Energy Regulator (AER, 2022) asserted that this earthquake was not induced, but a natural tectonic event. This assertion was based on preliminary depth estimates and a presumed lack of nearby operations. Contrary to this, we argue that this event was most likely induced.

Earthquakes induced by human activities are well documented (Ellsworth, 2013; Schultz et al., 2020) and have been of growing concern. The Western Canada Sedimentary Basin (WCSB) has had a long history of seismicity related to petroleum development. First, an older history related to conventional resource exploitation techniques of production, secondary recovery (Horner et al., 1994; Wetmiller, 1986), and wastewater disposal (Li et al., 2022; Schultz et al., 2014; Yu et al., 2022). Second, a recent surge in WCSB seismicity caused by unconventional development of shales via hydraulic fracturing (Atkinson et al., 2016). Typically, hydraulic fracturing of deeper shales has induced earthquakes: such as the Exshaw Formation (Schultz, Mei, et al., 2015), Duvernay Formation (Schultz & Wang, 2020; Wang et al., 2020), the Montney Formation (Mahani et al., 2017; Peña Castro

Project Administration: William L. Ellsworth
Resources: Ryan Schultz, William L. Ellsworth, Howard Zebkar, Paul Segall, Yu Jeffrey Gu, Sergey Samsonov
Software: Ryan Schultz, Jeong-Ung Woo, Karissa Pepin, William L. Ellsworth, Paul Segall, Sergey Samsonov
Supervision: Ryan Schultz, William L. Ellsworth, Howard Zebkar, Paul Segall
Validation: Ryan Schultz
Visualization: Ryan Schultz, Jeong-Ung Woo, Karissa Pepin, William L. Ellsworth
Writing – original draft: Ryan Schultz
Writing – review & editing: Ryan Schultz, Jeong-Ung Woo, Karissa Pepin, William L. Ellsworth, Paul Segall, Yu Jeffrey Gu

et al., 2020), and the Muskwa Shale. To date, both conventional and unconventional development have induced moderate magnitude events (M4), with the largest single event being M_W 4.6 (Mahani et al., 2017).

Large magnitude ($M > 5$) earthquakes have been induced by hydraulic fracturing, wastewater disposal, and enhanced geothermal systems elsewhere in the world (Foulger et al., 2018). Sometimes, these earthquakes have caused economic and human losses. In response, moratoriums have been placed on resource development due to concerns of earthquake risk. Thus, induced earthquakes raise questions for effective risk management (Schultz et al., 2021a, 2021b). Especially since a climate conscious energy transition requires subsurface injection of CO_2 at scale (Krevor et al., 2023). Therefore, a detailed analysis of the Peace River earthquakes is important for ensuring safe subsurface injection practices moving forward—especially considering the potential for CO_2 storage in Alberta (Zhang et al., 2022).

2. Background on In Situ Bitumen Recovery

Operations within the Peace River study area target the Bluesky Formation (Figure 1), a Lower Cretaceous aged glauconitic sandstone saturated with bitumen; initial estimates of in-place volume suggested approximately 10^{10} m^3 of oil sand hosted bitumen in the Peace River region (AER, 2015). Conventional bitumen recovery focuses on excavation in shallower basins; however, the Peace River region is too deep (~550–700 m) for economical excavation and instead utilizes unconventional in situ recovery techniques (Hein, 2017). Cyclic steaming stimulation (CSS), steam assisted gravity drainage (SAGD), and cold heavy oil production with sand (CHOPS) techniques are used to mobilize bitumen for extraction via well pumping (de Klerk, 2020). These unconventional recovery processes aim to decrease the viscosity of oil sands, for example, by injecting solvents or hot steam. Recovery typically produces a mixture of 25%–30% bitumen and 70%–75% water (de Klerk, 2020), which requires wastewater management via subsurface disposal. The study area has produced ~4.5×10^7 m^3 of oil and ~9.6×10^7 m^3 of water to date (~68% water). In response, ~1.0×10^8 m^3 of wastewater has been injected into basal sediments.

3. Peace River Earthquakes

We compile and reexamine seismicity in the Peace River study area dating back to 1985 (Gu et al., 2011; Schultz & Stern, 2015; Stern et al., 2013). The detectability of our catalog is temporally heterogenous, largely due to sparse station coverage and interrupted operation of nearby seismometers (Schultz, Stern, et al., 2015). Consequently, the seismic history of the region lacks the location resolution needed to precisely define fault structures. Despite this shortcoming, recent records define three separate areas of clustered earthquakes (north, middle, and south), two of which (middle and south) coincide with ongoing in situ bitumen recovery (Figure 1). These two clusters are relatively recent, (apparently) starting after station installations (mid-2014); there are also nearby deep injection wells disposing wastewater from bitumen recovery. The northern cluster is the longest and most persistent—identified immediately following installation of regional/local stations in 2014 (Figure 2). Almost certainly, this sequence initiated before it was detected. The southern cluster contains swarms of 18 $M > 2$ events that were first recorded in 2017. The most recent swarm started 23 November 2022, paused briefly, and then continued on 30 November with foreshocks of M_L 4.8 and 5.0 before rupturing the M_L 5.6 event. We note that a prior swarm also occurred here in mid-2021. Events trend along −47°, which is suggestive of a fault strike orientation. Eleven southern cluster earthquakes were large enough to determine moment tensors and centroid depths using the generalized cut-and-paste method (Figure 3 and Table S4 in Supporting Information S1). These earthquakes all have reverse mechanism, striking at ~NW-SE, with centroid depths of ~3.9 km. Our modeling constrains the 30 November 2022 event to M_W 5.1 with a centroid depth of ~4.0 km.

The southern cluster earthquakes produced surface deformation measurable by interferometric synthetic aperture radar (InSAR). The line of sight (LOS) ground displacement is confined to two lobes, with up to +3.4 cm and −0.8 cm of deformation between 18 and 30 November 2022 (Figure 3). The modeled fault slip is roughly circular (~2.0 km radius) with strike −63° and dip 58°; the peak slip (~29 cm) occurs at ~3.4 km depth. Our geodetically modeled moment (M_W 5.16, assuming a shear modulus of 30 GPa) is comparable to the seismically derived cumulative moment (M_W 5.13). Additional details on the processing of seismological and geodetic data can be found in Supporting Information S1 (Sections S1.1–S1.4).

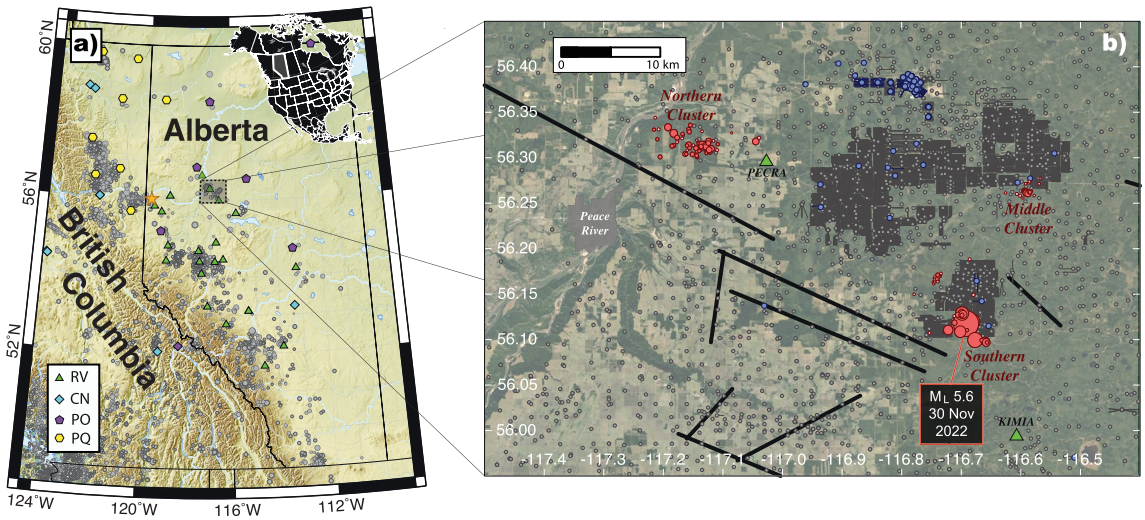

Figure 1. Study area and nearby industry operations. (a) Map showing the province of Alberta with regional seismicity (gray circles), the Dawson Creek M_W 5.4 earthquake (orange star), the study area (dotted box), and relevant stations (legend symbols) within ~500 km. Inset polygon shows the location of Alberta within North America. (b) Map showing the study area with earthquakes (red circles), nearby stations (green triangles), and the town of Peace River (gray polygon with text). Well locations are shown (gray tadpoles), with injection wells highlighted (blue tadpoles). Faults previously interpreted from stratigraphic offsets and 2D reflection seismic (Weides et al., 2014) are shown (black lines).

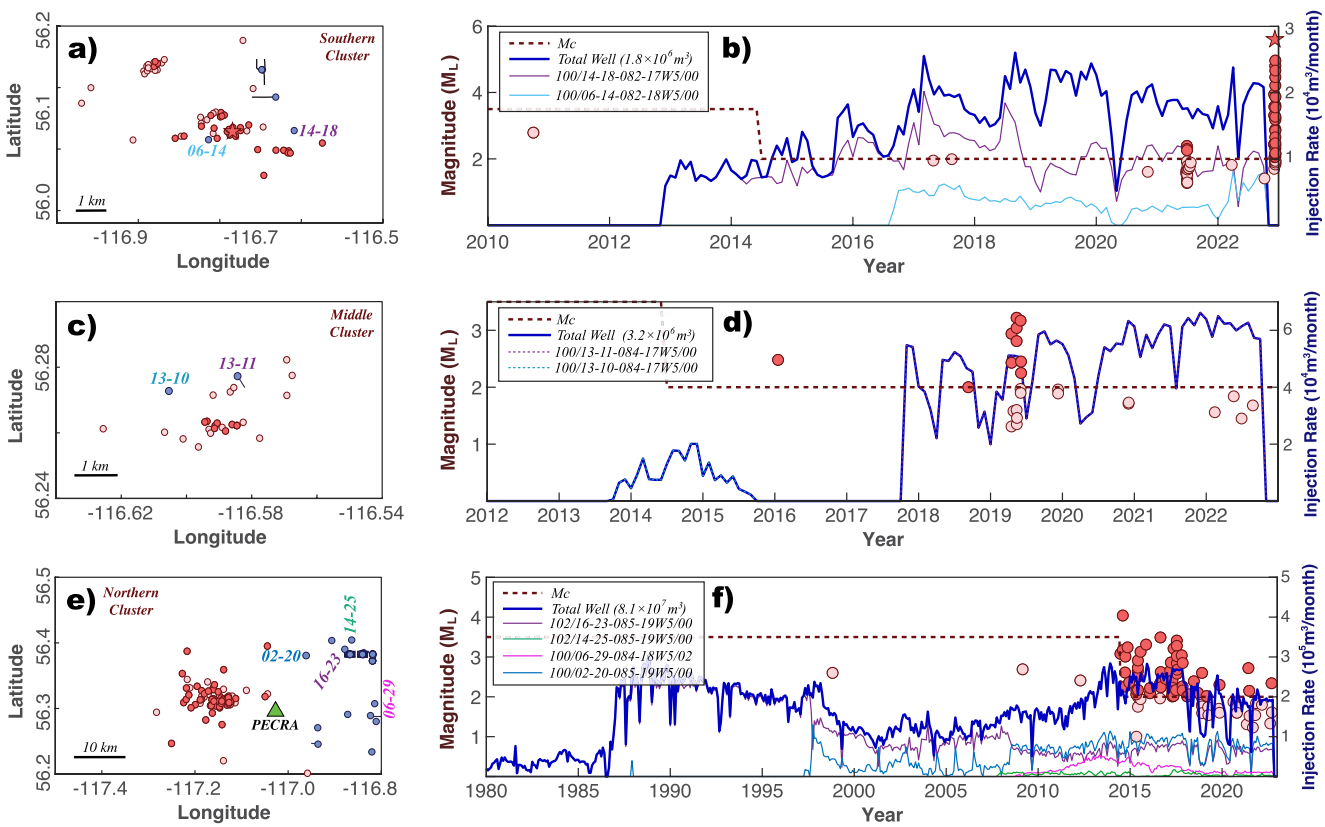

Figure 2. Space and time data for earthquakes and injection. Information for the three clusters near Peace River: South (top row), middle (middle row), and North (bottom row). The M_L 5.6 event is denoted by a red star. Left column (a, c, e) maps the earthquakes (red circles), injection wells (blue tadpoles and text), and stations (green triangles). Right column (b, d, f) temporally plots earthquake magnitudes (red circles), the magnitude of completeness (Mc, red dashed line), and monthly injection rates (blue lines). Earthquakes are distinguished for those above (darker red) and below (lighter red) the Mc. The inset legends show the color keys to the unique well identifier, with only deep (>1,750 m) and the few highest total volume (>10^5 m^3) disposal wells highlighted for clarity. The only exception is well 06–14 (792 m), due to its proximity to the M_L 5.6 event. Legends are partly transparent to allow viewing of timeseries data behind them.

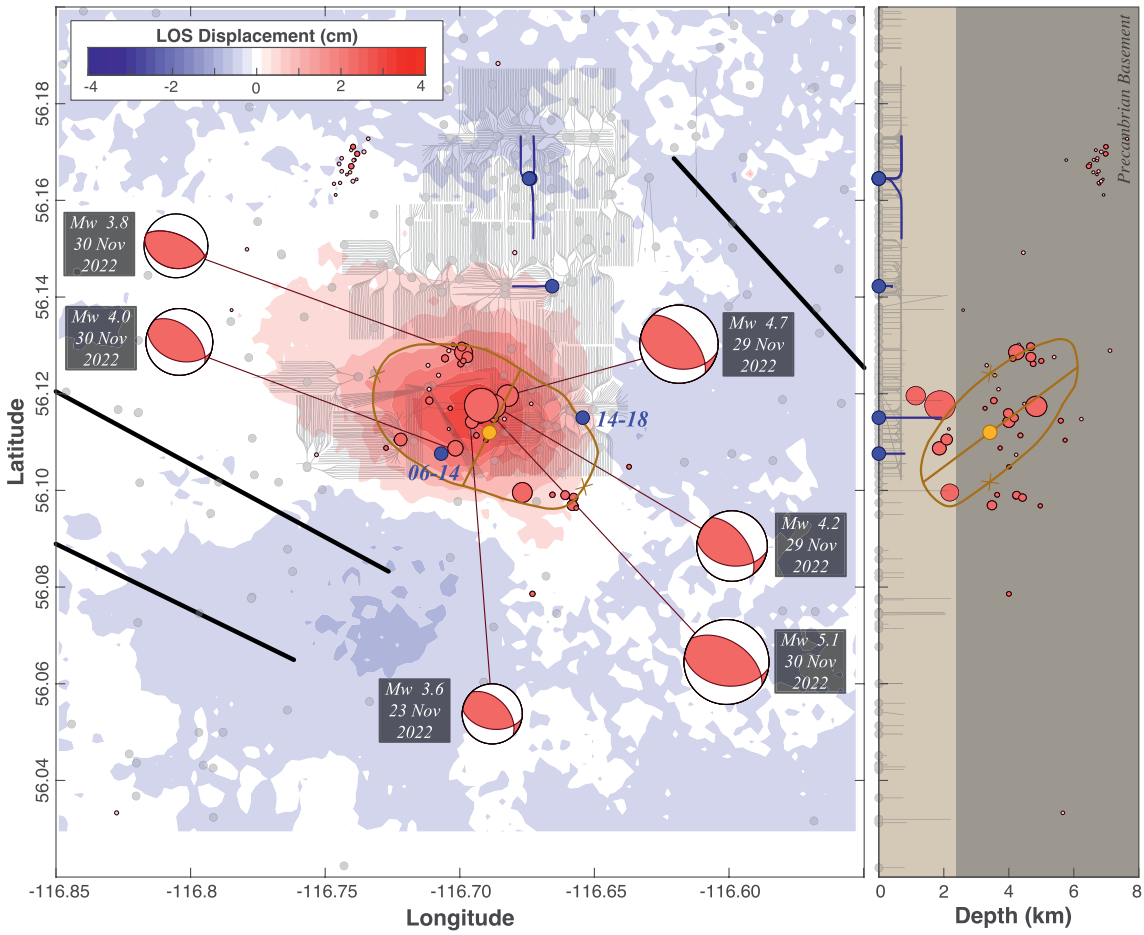

Figure 3. Local fault information comparison. Constraints on the reactivated fault in the southern cluster are compared for earthquake hypocenters (red circles), focal mechanisms (beach balls), geodetic slip extent (orange polygon), geodetic slip centroid (orange circle), and prior studies (black lines) (Weides et al., 2014). Geodetically modeled fault strike and dip orientations are indicated by the line between orange x's and the solid orange line, respectively. Additionally, well locations are provided (gray tadpoles) and highlighted for injection wells (blue tadpoles). Information is plotted in map view (left panel) and N-S depth profile (right panel). Colors represent InSAR ground displacement and colored depth profile indicates the depth of Precambrian basement.

4. Relationship to the Nearby Bitumen Recovery

The preliminary statement from the Alberta Energy Regulator (AER, 2022) said that this event was likely of natural/tectonic origin—rationalized by a lack of hydraulic fracturing activity, lack of nearby fluid disposal, and the depth of the earthquake. These rationalizations are contrary to the results of our study (Figures 2 and 3). To elaborate, we frame our discussion around the criteria for assessing if an earthquake has been induced (Foulger et al., 2022). These assessment criteria encompass an examination of the location/timing of the events with respect to the suspected operations, establishing a plausible means of communication between the operation and the reactivated fault, and assessing a mechanism for sufficient stress changes on the fault.

4.1. Spatiotemporal Association With Operations

Each of the three clusters in the Peace River region are examined for their spatiotemporal association with nearby disposal operations (Figure 2). Earthquakes in both the middle and southern cluster are relatively new and nearby deep disposal operations of significant volume.

For example, the middle cluster's centroid is ~1.5 km from well 13-11, which injected 10^6 m^3 of wastewater at 2.2 km depth into the Paleozoic aged Leduc Formation; seismicity initiated ~1.0–1.5 years after the initial injection and continues (Figures 2c and 2d). A more rigorous correlation analysis between the earthquake-injection time series indicates between 89% and 97% confidence of a temporal association (Section S1.5 and Figure S6 in

Supporting Information S1), which is suggestive of a causal relationship; although, this analysis is hampered by current data availability.

Similarly, the southern cluster's centroid is ∼2.3 km from well 14–18, which injected 10^6 m^3 of wastewater at 1.9 km depth into the Leduc Formation; seismicity appears to follow ∼4.5–8.5 years after the initial injection and occurs in swarms of activity (Figures 2a and 2b). The M_L 5.6 event occurs ∼10 years after injection at well 14–18 first started.

These distances and time delays are consistent with prior observations of induced seismicity, where delays are often on the order of years per kilometer (Ake et al., 2005; Park et al., 2020; Schultz et al., 2014; Wetmiller, 1986). These delays are often interpreted as the time required for the diffusion of pore pressure from the deep injection well, through the permeable aquifer, and along the fractured damage zone of a fault—until pressure increases are sufficient for fault slip reactivation (Ellsworth, 2013; Raleigh et al., 1976). The volumes injected in these disposal wells is comparable to (or greater than) prior induced seismicity cases within the WCSB (Li et al., 2022; Schultz et al., 2014).

The furthest, oldest, and most prolific cluster occurs north of Peace River (Figures 2e and 2f). The centroid of this cluster is ∼19 km from well 16–23, which injected more than 10^7 m^3 of wastewater at 1.9 km depth into the Leduc Formation since 1986. While well 16–23 is the most significant and long-duration injector, more than 10^6 m^3 of wastewater have been injected within the near-basement Paleozoic strata (1.8–1.9 km depths) in three other wells within 14–21 km. In total, almost 10^8 m^3 of wastewater has been disposed of in the vicinity of the northern cluster. Though we are unable to discern when seismicity started, due to poor network detection resolution prior to the 2014 improvements (Schultz, Stern, et al., 2015). Earthquakes were detected immediately following the installation of regional stations (Figure 2f). Therefore, it is likely that these northern earthquakes had already been ongoing (and undetected) for decades. Similarly, in the broader northern Alberta region, prior seismicity of significant magnitude (M 5.1) has been documented—and speculated to be induced, but this is inconclusive due to poorer station coverage (Milne, 1970).

In comparison to the Delaware Basin of west Texas, hydrological modelling suggests pore pressure increases on the order of 0.1–1 MPa (that are sufficient to initiate fault slip) can be transmitted at large distances (Ge et al., 2022). More directly, disposal induced earthquakes in the Delaware Basin have been caused from wells 25–40 km distant from the earthquake cluster (and injecting ∼10^{5-6} m^3 each) (Pepin et al., 2022; Skoumal et al., 2020). If induced, this northern cluster near Peace River would more closely resemble American cases of disposal earthquakes (that are induced by a network of wells over longer distances (McGarr & Barbour, 2017; Skoumal et al., 2020)) rather than the Canadian counterpart of more spatially restricted well-earthquake cases (Li et al., 2022; Schultz et al., 2014; Yu et al., 2022). Of course, the interpretation of these sequences as induced would require the existence of a critically stressed basement-rooted fault capable of hosting slip.

4.2. Relationship to Known Faults

The Peace River Arch (PRA) was a Paleozoic cratonic uplift associated with a passive margin that overprinted on the preexisting Precambrian basement structure; the PRA subsequently underwent extension until the Mesozoic, creating graben structures and an embayment (later a deep basin) (O'Connell et al., 1990). The lateral extent of the PRA is ∼140 km wide, extending for hundreds of kilometers basinward (east) from the Cordillera—it is one of the largest tectonic structures to influence the overlying sediments within the WCSB. Induced seismicity has already been documented in regions associated with PRA-related tectonic structures (Horner et al., 1994; Peña Castro et al., 2020). Our study area is situated in the eastern region of the PRA (Figure 1b), where normal faults of up to 40 km in strike length crosscut from basement into the sedimentary section (Weides et al., 2014). Local basement depths are reported to vary between 1.6 and 2.4 km (Weides et al., 2014).

Our composite analysis from earthquake relocations, focal mechanism inversions, and InSAR geodetic modeling paint a consistent picture of the seismicity in the southern cluster (Figure 3). For example, all three methodologies indicate the presence of a fault striking ∼NW-SE with centroid depths of 3.4–4.0 km. Geodetic inversions suggest that fault slip was predominantly in the basement, with a smaller fraction possibly extending into basal sediments up to ∼1.5 km in depth. Similarly, prior literature examining 2D reflection seismic and geophysical logs identified basement-rooted normal faults crosscutting the sedimentary section into the Late Cretaceous (Weides et al., 2014)—an interval that contains the target formation for in situ bitumen recovery. One of these previously

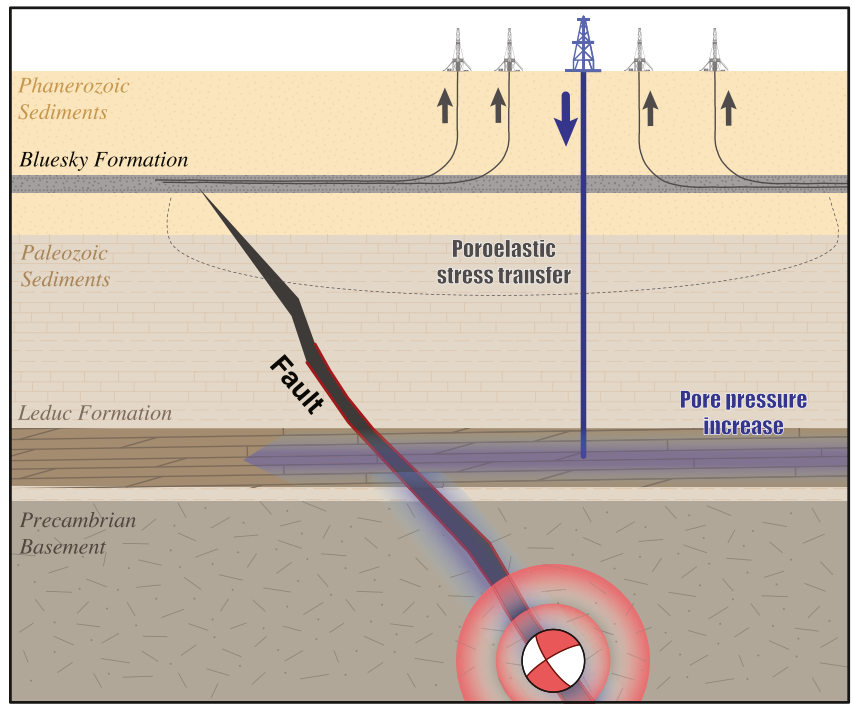

Figure 4. Interpreted triggering mechanisms. Bitumen recovery occurs from in situ wells (gray rigs and lines) targeting the Bluesky Formation (gray rectangle). The production of bitumen reduces overburden stress and increases horizontal stress (gray dashed line), which is transferred through the rock matrix, destabilizing the underlying fault (black line). As well, produced water is disposed of via injection wells (blue rig and line) targeting deep Paleozoic strata, like the Leduc Formation. The injection of fluids eventually increases pore pressure within the underlying fault, destabilizing it. The induced reverse fault slip (beachball) heaves the overlying strata, creating the InSAR observed ground deformation.

identified normal faults is close to the fault inferred in this paper. Such faults could provide a plausible means for channelized pore pressure migration from the basal Paleozoic injection interval (1.9 km) into the basement (<2.4 km). The deposition of basal carbonate reef formations, like the injected Leduc Formation, have (arguably) been influenced by faulting/tectonic structures (Corlett et al., 2018). Depth differentials of ~2–4 km between the sedimentary injection interval and basement induced earthquakes have been documented before (McGarr & Barbour, 2017; Schultz et al., 2014; Skoumal et al., 2020).

While reverse slip on our focal mechanism fault plane is expected for the WCSB stress field (Shen et al., 2019; Wang et al., 2018), the exact state of stress and structure that was reactivated in the 30 November 2022 M_L 5.6 (M_W 5.1) can be argued. Prior stress assessment suggested that the seismically resolved sedimentary normal faults were unlikely to be reactivated in a strike-slip regime (Weides et al., 2014). Correspondingly, much of the WCSB induced earthquakes have been strike-slip faulting in basal sediments (Shen et al., 2019; Wang et al., 2018). However, reverse faulting seismicity has been observed within the Precambrian basement (Schultz & Wang, 2020; Wetmiller, 1986)—suggesting either a stress regime bordering on strike-slip/reverse, or a depth dependent change in stress regime (Lund Snee & Zoback, 2020). It is worth noting that ancient normal faults reactivating with reverse slip in a modern stress field have been documented in other cases of induced seismicity (Clarke et al., 2014). Regardless of the exact structure hosting slip within the shallow basement, faults appear to have facilitated fluid pressure migration into the basement, inducing/triggering slip nucleation (Figure 4).

4.3. Appraisal of Triggering Mechanisms

Pore pressure increases are the most common mechanism for inducing seismicity: increasing pressure within a fault decreases the effective normal stress, perturbing the fault closer to the slip criteria (Raleigh et al., 1976). While we have focused on pore pressure increases due to wastewater injection, poroelastic stress changes from production are also known to cause fault slip initiation (Segall, 1989; Segall & Lu, 2015). Mass and volume reduction within the reservoir alters the stress state locally—promoting reverse slip above/below the reservoir

and normal slip at the margins. In fact, reverse earthquakes have already been induced on faults below a (secondary) production reservoir in the WCSB (Wetmiller, 1986). There, decades of production from the basal Leduc Formation in the Strachan D3A pool simultaneously reduced the overburden stress and increased the maximum horizontal stress: continued production (and subsequently continued stress magnitude changes) eventually reactivated a ∼1 km underlying basement fault after ∼5 years of gas extraction (Baranova et al., 1999).

Analogously, poroelastic stresses due to in situ bitumen recovery near Peace River would contribute to destabilizing an underlying basement fault for reverse reactivation. In this sense, there are multiple contributing mechanisms (pore pressure and poroelasticity) to fault reactivation (Figure 4). Here, we argue that pore pressure is likely the dominant mechanism. The first piece of evidence is from the northern cluster (Figures 1 and 2), which has no nearby in situ bitumen recovery; thus, this cluster's triggering mechanism must be entirely caused by long-range disposal effects. By analogy, it is plausible that a similar mechanism could be relevant for the middle and southern clusters. The second piece of evidence comes from estimates of the stress changes at the earthquake centroid from bitumen recovery (Figures S7–S8 and Section S1.6 in Supporting Information S1); this analysis suggests that stress changes from overburden removal and reservoir pressure decline would be (at most) on the order of 0.1–1 kPa, which is similar in magnitude to tidal stressing changes that only have arguable influences on triggering earthquakes (Yan et al., 2022). Typically, Coulomb failure stress changes on the order of 0.1–1 MPa are required to induce slip (Baranova et al., 1999; Ge et al., 2022). However, we acknowledge that a full thermo-hydromechanical modeling study would be required to assert the relative fault stress changes more confidently; especially since there are cases of induced seismicity where both production and disposal likely contributed to fault reactivation (Grasso et al., 2021). We also note that once the earthquakes have begun, earthquake-earthquake interactions could also impact the distribution of stress on the fault (Wang et al., 2020).

4.4. Implications

Addressing climate change, while also allowing the petroleum industry to operate, will require the successful development of blue hydrogen and/or CO_2 storage at scale. Blue hydrogen—the synthesis of hydrogen as a fuel from heavy oil or bitumen—creates CO_2 as a byproduct, which must be sequestered by subsurface injection. Industrial scale injection of CO_2 into deep sedimentary formations carries similar risks of inducing earthquakes as wastewater disposal (Zoback & Gorelick, 2012), with some subtle differences to account for multiphase fluid flow and CO_2 dissolution (Vilarrasa & Carrera, 2015). Consideration of CO_2 injection and blue hydrogen will likely be important for the future of industry in Alberta (Krevor et al., 2023; Razi & Dincer, 2022; Zhang et al., 2022).

Injection of fluids into the subsurface is currently seen as the most economical means to dispose of industrial waste. Safe injection of CO_2 will require an understanding of fault reactivation potential, derived from geomechanics and in situ measurement of pressures and stresses, as well as high-sensitivity monitoring for seismicity during the lifetime of the project (Templeton et al., 2023). Forward thinking CO_2 development can learn two things from the Peace River case. First, that long-term operations (including subsurface injection) have the potential to induce earthquakes—often with significant lag times for seismic response. Second, the importance of high sensitivity measurement both before and during the lifetime of the project: here, the lack of precise and low-magnitude seismic data hampered the resolvability of induced events and their properties. These lessons are particularly important considering the significant potential of low b-values (0.55 ± 0.05 observed here) for large magnitude events (Figure S1 in Supporting Information S1), exponential scaling of consequence with magnitude (Langenbruch et al., 2020), and the influence of location on exposure to risk (Schultz et al., 2021a, 2021b). Certainly, other $M > 5$ induced events (in highly exposed locations) have caused damage and ended operations (Foulger et al., 2018). Ideally, operations would be sited in locations that are remote from critical infrastructure, residential homes, and industrial operations—to balance the earthquake consequences with the costs/risks of waste transportation. These considerations will be key to monitoring injection, understanding induced earthquakes, planning for sustainable/safe injection practices, and developing mitigation/management strategies for their hazards and risks.

5. Conclusions

Contrary to previous assessments, we find that the M_L 5.6 (M_W 5.1) 30 November 2022 event was most likely induced—highlighting the importance of rigorous causation assessment. Our conclusion is based on a

spatiotemporal assessment of earthquakes with nearby injection, evidence of nearby normal faults from the Peace River Arch, viable triggering mechanisms, and a contextual comparison against prior induced cases. We interpret that wastewater from in situ bitumen recovery disposed into basal Paleozoic sediments increased aquifer pore pressures, that diffused to pre-existing (normal) faults, channelizing downwards along the fault damage zone (or other pathways), increasing fault pressures until reaching the critical slip criteria. The fault reactivated in reverse due to the orientation and magnitudes of the current stress field. While pore pressure increases are the likely culprit for triggering these events, poroelastic contributions from in situ bitumen recovery may have also played a subtle role in promoting fault slip. Examination of two other Peace River sequences would suggest that they were similarly induced—with one potentially ongoing and undetected in the past. The results of this study will have implications for future industry development, such as CO_2 storage and blue hydrogen.

Data Availability Statement

The derived catalogue (Table S1), phase picks (Table S2), and focal mechanism (Table S4 in Supporting Information S1) are available as supplements. Regional waveform data is from several networks including: the Regional Alberta Observatory for Earthquake Studies Network (Schultz & Stern, 2015) (https://doi.org/10.7914/SN/RV), Canadian Rockies and Alberta Network (Gu et al., 2011), Canadian National Seismic Network (https://doi.org/10.7914/SN/CN), and Portable Observatories for Lithospheric Analysis and Research Investigating Seismicity. All waveform data is publicly available online at the Incorporated Research Institutions for Seismology (IRIS). Regional catalogue information from the Alberta Geological Survey (Stern et al., 2013) is available online (https://ags-aer.shinyapps.io/Seismicity_waveform_app/). Regional catalogue information from Natural Resources Canada is also available online (https://earthquakescanada.nrcan.gc.ca/stndon/NEDB-BNDS/bulletin-en.php). Local information on faulting were digitized from prior work (Weides et al., 2014). The Sentinel-1 InSAR data used in this study is publicly available for download at the European Space Agency's Open Access Hub (https://scihub.copernicus.eu/dhus/#/home) or from the Alaska Satellite Facility's online Vertex (https://search.asf.alaska.edu/#/). Industry well information including production and injection activities were accessed through Prism via Enervus (https://www.enverus.com/).

Acknowledgments
Funding for this work came from the Stanford Center for Induced and Triggered Seismicity. The authors would like to thank two anonymous reviewers for their comments that helped improve this manuscript.

References

AER, Alberta Energy Regulator. (2015). ST98-2015. Alberta's energy reserves 2014 and supply/demand outlook 2015–2024 (p. 299). Retrieved from https://static.aer.ca/prd/documents/sts/ST98/ST98-2015.pdf

AER, Alberta Energy Regulator. (2022). Seismic events southeast of Peace River. Announcement - November 30, 2022. Retrieved from https://www.aer.ca/providing-information/news-and-resources/news-and-announcements/announcements/announcement-november-30-2022

Ake, J., Mahrer, K., O'Connell, D., & Block, L. (2005). Deep-injection and closely monitored induced seismicity at Paradox Valley, Colorado. *Bulletin of the Seismological Society of America*, *95*(2), 664–683. https://doi.org/10.1785/0120040072

Atkinson, G. M., Eaton, D. W., Ghofrani, H., Walker, D., Cheadle, B., Schultz, R., et al. (2016). Hydraulic fracturing and seismicity in the Western Canada Sedimentary Basin. *Seismological Research Letters*, *87*(3), 631–647. https://doi.org/10.1785/0220150263

Baranova, V., Mustaqeem, A., & Bell, S. (1999). A model for induced seismicity caused by hydrocarbon production in the Western Canada Sedimentary Basin. *Canadian Journal of Earth Sciences*, *36*(1), 47–64. https://doi.org/10.1139/e98-080

Clarke, H., Eisner, L., Styles, P., & Turner, P. (2014). Felt seismicity associated with shale gas hydraulic fracturing: The first documented example in Europe. *Geophysical Research Letters*, *41*(23), 8308–8314. https://doi.org/10.1002/2014GL062047

Corlett, H., Schultz, R., Branscombe, P., Hauck, T., Haug, K., MacCormack, K., & Shipman, T. (2018). Subsurface faults inferred from reflection seismic, earthquakes, and sedimentological relationships: Implications for induced seismicity in Alberta, Canada. *Marine and Petroleum Geology*, *93*, 135–144. https://doi.org/10.1016/j.marpetgeo.2018.03.008

de Klerk, A. (2020). Unconventional oil: Oilsands. In *Future energy* (pp. 49–65). Elsevier. https://doi.org/10.1016/B978-0-08-102886-5.00003-7

Ellsworth, W. L. (2013). Injection-induced earthquakes. *Science*, *341*(6142). https://doi.org/10.1126/science.1225942

Foulger, G. R., Wilkinson, M. W., Wilson, M. P., Gluyas, J. G., & Tezel, T. (2022). Human-induced earthquakes: E-PIE – A generic tool for evaluating proposals of induced earthquakes. *Journal of Seismology*, *27*(1), 21–44. https://doi.org/10.1007/s10950-022-10122-8

Foulger, G. R., Wilson, M. P., Gluyas, J. G., Julian, B. R., & Davies, R. J. (2018). Global review of human-induced earthquakes. *Earth-Science Reviews*, *178*, 438–514. https://doi.org/10.1016/j.earscirev.2017.07.008

Ge, J., Nicot, J. P., Hennings, P. H., Smye, K. M., Hosseini, S. A., Gao, R. S., & Breton, C. L. (2022). Recent water disposal and pore pressure evolution in the Delaware Mountain Group, Delaware Basin, southeast New Mexico and West Texas, USA. *Journal of Hydrology: Regional Studies*, *40*, 101041. https://doi.org/10.1016/j.ejrh.2022.101041

Grasso, J. R., Amorese, D., & Karimov, A. (2021). Did wastewater disposal drive the longest seismic swarm triggered by fluid manipulations? Lacq, France, 1969–2016. *Bulletin of the Seismological Society of America*, *111*(5), 2733–2752. https://doi.org/10.1785/0120200359

Gu, Y. J., Okeler, A., Shen, L., & Contenti, S. (2011). The Canadian Rockies and Alberta network (CRANE): New constraints on the Rockies and western Canada sedimentary basin. *Seismological Research Letters*, *82*(4), 575–588. https://doi.org/10.1785/gssrl.82.4.575

Hein, F. J. (2017). Geology of bitumen and heavy oil: An overview. *Journal of Petroleum Science and Engineering*, *154*, 551–563. https://doi.org/10.1016/j.petrol.2016.11.025

Horner, R. B., Barclay, J. E., & MacRae, J. M. (1994). Earthquakes and hydrocarbon production in the Fort St. John area of northeastern British Columbia. *Canadian Journal of Exploration Geophysics*, *30*(1), 39–50.

Krevor, S., de Conick, H., Gasda, S. E., Ghaleigh, N. S., de Gooyert, V., Hajibeygi, H., et al. (2023). Subsurface carbon dioxide and hydrogen storage for a sustainable energy future. *Nature Reviews Earth & Environment*, *4*(2), 102–118. https://doi.org/10.1038/s43017-022-00376-8

Langenbruch, C., Ellsworth, W. L., Woo, J. U., & Wald, D. J. (2020). Value at induced risk: Injection-induced seismic risk from low-probability, high-impact events. *Geophysical Research Letters*, *47*(2), e2019GL085878. https://doi.org/10.1029/2019GL085878

Li, T., Gu, Y. J., Wang, J., Wang, R., Yusifbayov, J., Canales, M. R., & Shipman, T. (2022). Earthquakes induced by wastewater disposal near Musreau Lake, Alberta, 2018–2020. *Bulletin of the Seismological Society of America*, *93*(2A), 727–738. https://doi.org/10.1785/0220210139

Lund Snee, J. E., & Zoback, M. D. (2020). Multiscale variations of the crustal stress field throughout North America. *Nature Communications*, *11*(1), 1–9. https://doi.org/10.1038/s41467-020-15841-5

Mahani, A. B., Schultz, R., Kao, H., Walker, D., Johnson, J., & Salas, C. (2017). Fluid injection and seismic activity in the northern Montney play, British Columbia, Canada, with special reference to the 17 August 2015 M w 4.6 induced earthquake. *Bulletin of the Seismological Society of America*, *107*(2), 542–552. https://doi.org/10.1785/0120160175

McGarr, A., & Barbour, A. J. (2017). Wastewater disposal and the earthquake sequences during 2016 near Fairview, Pawnee, and Cushing, Oklahoma. *Geophysical Research Letters*, *44*(18), 9330–9336. https://doi.org/10.1002/2017GL075258

Milne, W. G. (1970). The Snipe Lake, Alberta earthquake of March 8, 1970. *Canadian Journal of Earth Sciences*, *7*(6), 1564–1567. https://doi.org/10.1139/e70-148

O'Connell, S. C., Dix, G. R., & Barclay, J. E. (1990). The origin, history, and regional structural development of the Peace River Arch, Western Canada. *Bulletin of Canadian Petroleum Geology*, *38*(1), 4–24. https://doi.org/10.35767/gscpgbull.38a.1.004

Park, Y., Mousavi, S. M., Zhu, W., Ellsworth, W. L., & Beroza, G. C. (2020). Machine-learning-based analysis of the Guy-Greenbrier, Arkansas earthquakes: A tale of two sequences. *Geophysical Research Letters*, *47*(6), e2020GL087032. https://doi.org/10.1029/2020GL087032

Peña Castro, A. F., Roth, M. P., Verdecchia, A., Onwuemeka, J., Liu, Y., Harrington, R. M., et al. (2020). Stress chatter via fluid flow and fault slip in a hydraulic fracturing-induced earthquake sequence in the Montney Formation, British Columbia. *Geophysical Research Letters*, *47*(14), e2020GL087254. https://doi.org/10.1029/2020GL087254

Pepin, K. S., Ellsworth, W. L., Sheng, Y., & Zebker, H. A. (2022). Shallow aseismic slip in the Delaware basin determined by Sentinel-1 InSAR. *Journal of Geophysical Research: Solid Earth*, *127*(2), e2021JB023157. https://doi.org/10.1029/2021JB023157

Raleigh, C. B., Healy, J. H., & Bredehoeft, J. D. (1976). An experiment in earthquake control at Rangely, Colorado. *Science*, *191*(4233), 1230–1237. https://doi.org/10.1126/science.191.4233.1230

Razi, F., & Dincer, I. (2022). Challenges, opportunities, and future directions in hydrogen sector development in Canada. *International Journal of Hydrogen Energy*, *47*(15), 9083–9102. https://doi.org/10.1016/j.ijhydene.2022.01.014

Schultz, R., Beroza, G. C., & Ellsworth, W. L. (2021a). A risk-based approach for managing hydraulic fracturing–induced seismicity. *Science*, *372*(6541), 504–507. https://doi.org/10.1126/science.abg5451

Schultz, R., Beroza, G. C., & Ellsworth, W. L. (2021b). A strategy for choosing red-light thresholds to manage hydraulic fracturing induced seismicity in North America. *Journal of Geophysical Research: Solid Earth*, *126*(12), e2021JB022340. https://doi.org/10.1029/2021JB022340

Schultz, R., Mei, S., Pană, D., Stern, V., Gu, Y. J., Kim, A., & Eaton, D. (2015). The Cardston earthquake swarm and hydraulic fracturing of the exshaw formation (Alberta Bakken Play). *Bulletin of the Seismological Society of America*, *105*(6), 2871–2884. https://doi.org/10.1785/0120150131

Schultz, R., Skoumal, R., Brudzinski, M., Eaton, D., Baptie, B., & Ellsworth, W. (2020). Hydraulic fracturing induced seismicity. *Reviews of Geophysics*, *58*(3), e2019RG000695. https://doi.org/10.1029/2019RG000695

Schultz, R., & Stern, V. (2015). The regional Alberta observatory for earthquake studies network (RAVEN). *CSEG Recorder*, *40*(8), 34–37.

Schultz, R., Stern, V., & Gu, Y. J. (2014). An investigation of seismicity clustered near the Cordel Field, west central Alberta, and its relation to a nearby disposal well. *Journal of Geophysical Research: Solid Earth*, *119*(4), 3410–3423. https://doi.org/10.1002/2013JB010836

Schultz, R., & Wang, R. (2020). A newly emerging case of hydraulic fracturing induced seismicity in the Duvernay East Shale Basin. *Tectonophysics*, *779*, 228393. https://doi.org/10.1016/j.tecto.2020.228393

Schultz, R., Stern, V., Gu, Y. J., & Eaton, D. (2015). Detection threshold and location resolution of the Alberta Geological Survey earthquake catalogue. *Seismological Research Letters*, *86*(2A), 385–397. https://doi.org/10.1785/0220140203

Segall, P. (1989). Earthquakes triggered by fluid extraction. *Geology*, *17*(10), 942–946. https://doi.org/10.1130/0091-7613(1989)017<0942:ETBFE>2.3.CO;2

Segall, P., & Lu, S. (2015). Injection-induced seismicity: Poroelastic and earthquake nucleation effects. *Journal of Geophysical Research: Solid Earth*, *120*(7), 5082–5103. https://doi.org/10.1002/2015JB012060

Shen, L. W., Schmitt, D. R., & Schultz, R. (2019). Frictional stabilities on induced earthquake fault planes at Fox Creek, Alberta: A pore fluid pressure dilemma. *Geophysical Research Letters*, *46*(15), 8753–8762. https://doi.org/10.1029/2019GL083566

Skoumal, R. J., Barbour, A. J., Brudzinski, M. R., Langenkamp, T., & Kaven, J. O. (2020). Induced seismicity in the Delaware basin, Texas. *Journal of Geophysical Research: Solid Earth*, *125*(1), e2019JB018558. https://doi.org/10.1029/2019JB018558

Stern, V. H., Schultz, R. J., Shen, L., Gu, Y. J., & Eaton, D. W. (2013). Alberta earthquake catalogue, version 1.0, September 2006 through December 2010. Alberta Geological Survey Open–File Report (Vol. *15*, p. 36).

Templeton, D. C., Schoenball, M., Layland-Bachmann, C. E., Foxall, W., Guglielmi, Y., Kroll, K. A., et al. (2023). A project lifetime approach to the management of induced seismicity risk at geologic carbon storage sites. *Seismological Society of America*, *94*(1), 113–122. https://doi.org/10.1785/0220210284

Vilarrasa, V., & Carrera, J. (2015). Geologic carbon storage is unlikely to trigger large earthquakes and reactivate faults through which CO_2 could leak. *Proceedings of the National Academy of Sciences of the United States of America*, *112*(19), 5938–5943. https://doi.org/10.1073/pnas.1413284112

Wang, J., Li, T., Gu, Y. J., Schultz, R., Yusifbayov, J., & Zhang, M. (2020). Sequential fault reactivation and secondary triggering in the March 2019 Red Deer induced earthquake swarm. *Geophysical Research Letters*, *47*(22), e2020GL090219. https://doi.org/10.1029/2020GL090219

Wang, R., Gu, Y. J., Schultz, R., & Chen, Y. (2018). Faults and non-double-couple components for induced earthquakes. *Geophysical Research Letters*, *45*(17), 8966–8975. https://doi.org/10.1029/2018GL079027

Weides, S. N., Moeck, I. S., Schmitt, D. R., & Majorowicz, J. A. (2014). An integrative geothermal resource assessment study for the siliciclastic Granite Wash Unit, northwestern Alberta (Canada). *Environmental Earth Sciences*, *72*(10), 4141–4154. https://doi.org/10.1007/s12665-014-3309-3

Wetmiller, R. J. (1986). Earthquakes near Rocky Mountain House, Alberta, and their relationship to gas production facilities. *Canadian Journal of Earth Sciences*, *23*(2), 172–181. https://doi.org/10.1139/e86-020

Yan, R., Chen, X., Sun, H., Xu, J., & Zhou, J. (2022). A review of tidal triggering of global earthquakes. *Geodesy and Geodynamics*, *14*(1), 35–42. https://doi.org/10.1016/j.geog.2022.06.005

Yu, H., Kao, H., Wang, B., & Visser, R. (2022). Long-term fluid injection can expedite fault reactivation and development: Riedel shear structures illuminated by induced earthquakes in Alberta, Canada. *Journal of Geophysical Research: Solid Earth*, *127*(10), e2022JB025126. https://doi.org/10.1029/2022JB025126

Zhang, K., Lau, H. C., & Chen, Z. (2022). Regional carbon capture and storage opportunities in Alberta, Canada. *Fuel*, *322*, 124224. https://doi.org/10.1016/j.fuel.2022.124224

Zoback, M. D., & Gorelick, S. M. (2012). Earthquake triggering and large-scale geologic storage of carbon dioxide. *Proceedings of the National Academy of Sciences of the United States of America*, *109*(26), 10164–10168. https://doi.org/10.1073/pnas.120247310

References From the Supporting Information

Abrams, M., Crippen, R., & Fujisada, H. (2020). ASTER global digital elevation model (GDEM) and ASTER global water body dataset (ASTWBD). *Remote Sensing*, *12*(7), 1156. https://doi.org/10.3390/rs12071156

Battaglia, M., Cervelli, P. F., & Murray, J. R. (2013). Modeling crustal deformation near active faults and volcanic centers. *Journal of Volcanology and Geothermal Research*, *254*, 1–4. https://doi.org/10.1016/j.jvolgeores.2012.12.018

Beyreuther, M., Barsch, R., Krischer, L., Megies, T., Behr, Y., & Wassermann, J. (2010). ObsPy: A Python toolbox for seismology. *Seismological Research Letters*, *81*(3), 530–533. https://doi.org/10.1785/gssrl.81.3.530

Chen, C. W., & Zebker, H. A. (2001). Two-dimensional phase unwrapping with use of statistical models for cost functions in nonlinear optimization. *Journal of the Optical Society of America A*, *18*(2), 338–351. https://doi.org/10.1364/JOSAA.18.000338

Costantini, M. (1998). A novel phase unwrapping method based on network programming. *IEEE Transactions on Geoscience and Remote Sensing*, *36*(3), 813–821. https://doi.org/10.1109/36.673674

Fung, Y. C. (1965). *Foundations of solid mechanics* (pp. 195–197). Prentice-Hall.

Goldstein, R. M., & Werner, C. L. (1998). Radar interferogram filtering for geophysical applications. *Geophysical Research Letters*, *25*(21), 4035–4038. https://doi.org/10.1029/1998GL900033

Gutenberg, B., & Richter, C. F. (1956). Earthquake magnitude, intensity, energy, and acceleration. *Bulletin of the Seismological Society of America*, *46*(2), 105–145. https://doi.org/10.1785/bssa0460020105

Heimann, S., Kriegerowski, M., Isken, M., Cesca, S., Daout, S., Grigoli, F., et al. (2017). *Pyrocko-An open-source seismology toolbox and library*. GFZ Data Services. https://doi.org/10.5880/GFZ.2.1.2017.001

Kissling, E., Ellsworth, W. L., Eberhart-Phillips, D., & Kradolfer, U. (1994). Initial reference models in local earthquake tomography. *Journal of Geophysical Research*, *99*(B10), 19635–19646. https://doi.org/10.1029/93JB03138

Okada, Y. (1985). Surface deformation due to shear and tensile faults in a half-space. *Bulletin of the Seismological Society of America*, *75*(4), 1135–1154. https://doi.org/10.1785/BSSA0750041135

Schultz, R., & Telesca, L. (2018). The cross-correlation and reshuffling tests in discerning induced seismicity. *Pure and Applied Geophysics*, *175*(10), 3395–3401. https://doi.org/10.1007/s00024-018-1890-1

Waldhauser, F., & Ellsworth, W. L. (2000). A double-difference earthquake location algorithm: Method and application to the northern Hayward fault, California. *Bulletin of the Seismological Society of America*, *90*(6), 1353–1368. https://doi.org/10.1785/0120000006

Wegmuller, U., & Werner, C. (1997). GAMMA SAR processor and interferometry software. In *Proceedings of the 3rd ERS symposium on space at the service of our environment* (pp. 14–21).

Yang, X. M., Davis, P. M., & Dieterich, J. H. (1988). Deformation from inflation of a dipping finite prolate spheroid in an elastic half-space as a model for volcanic stressing. *Journal of Geophysical Research*, *93*(B5), 4249–4257. https://doi.org/10.1029/JB093iB05p04249

Zhu, L., & Rivera, L. A. (2002). A note on the dynamic and static displacements from a point source in multilayered media. *Geophysical Journal International*, *148*(3), 619–627. https://doi.org/10.1046/j.1365-246X.2002.01610.x

Zhu, L., & Helmberger, D. V. (1996). Advancement in source estimation techniques using broadband regional seismograms. *Bulletin of the Seismological Society of America*, *86*(5), 1634–1641. https://doi.org/10.1785/BSSA0860051634